Apc modulates embryonic stem-cell differentiation by controlling the dosage of β-catenin signaling

Menno F. Kielman[1], Maaret Rindapää[1]*, Claudia Gaspar[1]*, Nicole van Poppel[1], Cor Breukel[1], Sandra van Leeuwen[1], Makoto Mark Taketo[2], Scott Roberts[3], Ron Smits[1] & Riccardo Fodde[1]

*These authors contributed equally to this work.

Published online 11 November 2002; doi:10.1038/ng1045

The Wnt signal-transduction pathway induces the nuclear translocation of membrane-bound β-catenin (Catnb) and has a key role in cell-fate determination. Tight somatic regulation of this signal is essential, as uncontrolled nuclear accumulation of β-catenin can cause developmental defects and tumorigenesis in the adult organism. The adenomatous polyposis coli gene (*APC*) is a major controller of the Wnt pathway and is essential to prevent tumorigenesis in a variety of tissues and organs. Here, we have investigated the effect of different mutations in *Apc* on the differentiation potential of mouse embryonic stem (ES) cells. We provide genetic and molecular evidence that the ability and sensitivity of ES cells to differentiate into the three germ layers is inhibited by increased doses of β-catenin by specific *Apc* mutations. These range from a severe differentiation blockade in *Apc* alleles completely deficient in β-catenin regulation to more specific neuroectodermal, dorsal mesodermal and endodermal defects in more hypomorphic alleles. Accordingly, a targeted oncogenic mutation in *Catnb* also affects the differentiation potential of ES cells. Expression profiling of wildtype and *Apc*-mutated teratomas supports the differentiation defects at the molecular level and pinpoints a large number of downstream structural and regulating genes. Chimeric experiments showed that this effect is cell-autonomous. Our results imply that constitutive activation of the Apc/β-catenin signaling pathway results in differentiation defects in tissue homeostasis, and possibly underlies tumorigenesis in the colon and other self-renewing tissues.

Introduction

Wnt signalling induces nuclear translocation of transcriptionally active β-catenin through interference with a multi-protein complex (composed of glycogen synthase kinase 3β (GSK3B), axin 1, axin 2 and APC) capable of earmarking free cytoplasmic β-catenin for degradation through the ubiquitin/proteasome pathway[1,2]. One of the key components of this complex is the APC tumor suppressor, which serves as the scaffold to which β-catenin, axin 1 and axin 2 bind[3]. Mutations in *APC* are responsible for familial adenomatous polyposis (FAP), an autosomal dominant predisposition to the development of hundreds to thousands of adenomatous polyps in the colon and rectum[4]. Moreover, mutations in *APC* initiate the majority of sporadic colorectal cancers[3,5].

Several mutated alleles of the mouse *Apc* gene have been generated (Fig. 1*a*). Notably, they result in different developmental defects and different degrees of tumor predisposition and incidence[6]. The Apc^{Min} allele encodes a stable truncated protein of 850 amino acids lacking all the β-catenin binding and downregulating motifs. Heterozygous $Apc^{+/Min}$ mice develop multiple intestinal tumors, whereas $Apc^{Min/Min}$ embryos die at very early developmental stages[7,8]. Two different *Apc* mouse models, Apc^{1638T} and Apc^{1638N}, were generated in our laboratory by introducing a selection cassette at codon 1638 of the endogenous *Apc* gene in the sense and anti-sense transcriptional orientation, respectively[9]. Heterozygous $Apc^{+/1638N}$ mice develop approximately 5–6 intestinal polyps in addition to a broad spectrum of extra-intestinal manifestations including desmoids, epidermal cysts, pilomatricomas and breast tumors[10,11]. Homozygosity with respect to the Apc^{1638N} allele is embryonic lethal[10,11]. In contrast, $Apc^{1638T/1638T}$ mice are viable and tumor-free[9].

Similar genotype–phenotype correlations have been established in humans between mutations in *APC* and the degree of severity of the corresponding FAP phenotype[12]. But the molecular and cellular mechanisms underlying these phenotypic differences are not understood. In fact, owing to the high complexity and turnover of the intestinal epithelium as a biological system, little is known regarding the cancer-causing cellular mechanisms

[1]*Center for Human and Clinical Genetics, Leiden University Medical Center, Sylvius Laboratory, Wassenaarseweg 72, 2333 RA Leiden, The Netherlands.* [2]*Department of Pharmacology, Kyoto University Graduate School of Medicine, Kyoto, Japan.* [3]*Rosetta Inpharmatics, Kirkland, Washington, USA. Correspondence should be addressed to R.F. (e-mail: r.fodde@lumc.nl).*

triggered by loss of APC function. Alterations in rates of proliferation, apoptosis, cell migration and differentiation have been postulated to be involved. The observation that loss of function of transcription factor 4 (Tcf4) in mice leads to the depletion of intestinal stem cells indicates a role of the Wnt/β-catenin signal-transduction pathway in epithelial stem-cell maintainance[13]. More recently, computer modeling studies implicated crypt stem-cell overproduction in tumor initiation in the colon[14].

Here, we analyzed the capacity of pluripotent stem cells carrying different *Apc* and *Catnb* alleles to differentiate into specialized cell lineages.

Results

Characterization of ES-cell lines with mutations in *Apc*

To elucidate the molecular basis of the phenotypic consequences of different mutations in *Apc* and to evaluate their effect on stem-cell differentiation, we generated different ES-cell lines carrying four mutated *Apc* alleles (Fig. 1*a*) in different combinations, and analyzed their expression level and β-catenin-driven transcriptional activity. ES-cell lines were generated either by two rounds of gene targeting[9] or by direct isolation from preimplantation blastocysts. We also analyzed Apc^{1527T}, a new allele obtained by deleting 197 nucleotides from the 3′ end of the original Apc^{1638T} targeting construct, thereby removing the only residual SAMP repeat (the axin-binding domain; ref. 9; Fig. 1*a*). Western-blot analysis showed that all the alleles except for Apc^{1638N} stably expressed the predicted truncated protein at a 1:1 ratio with the full-length wildtype protein (Fig. 1*b*). In contrast, no truncated protein was detected in heterozygous $Apc^{+/1638N}$ mice or ES cells (Fig. 1*b*).

To determine whether the Apc^{1638N} mutation represents a true null allele, we attempted to identify minimal amounts of the truncated protein in homozygous Apc^{1638N} cells by immunoprecipitation analysis (Fig. 1*c*). We observed a weak band of 182 kD (the size of the Apc^{1638T} truncated protein). We then quantified the truncated Apc protein relative to its full-length equivalent by competition immunoprecipitation assays, which indicated that the Apc^{1638N} allele expressed the mutant protein at approximately 2% of the endogenous level in ES cells (Fig. 1*c*). Therefore, the Apc^{1638N} mutation represents a leaky hypomorphic variant of the Apc^{1638T} allele.

The differences in expression levels of truncated Apc proteins were reflected by the corresponding levels of transcriptionally active nuclear β-catenin measured by the TCF/β-catenin responsive reporter assay TOPFLASH[15]. Previous analysis showed an increasing gradient of β-catenin regulatory activity among the

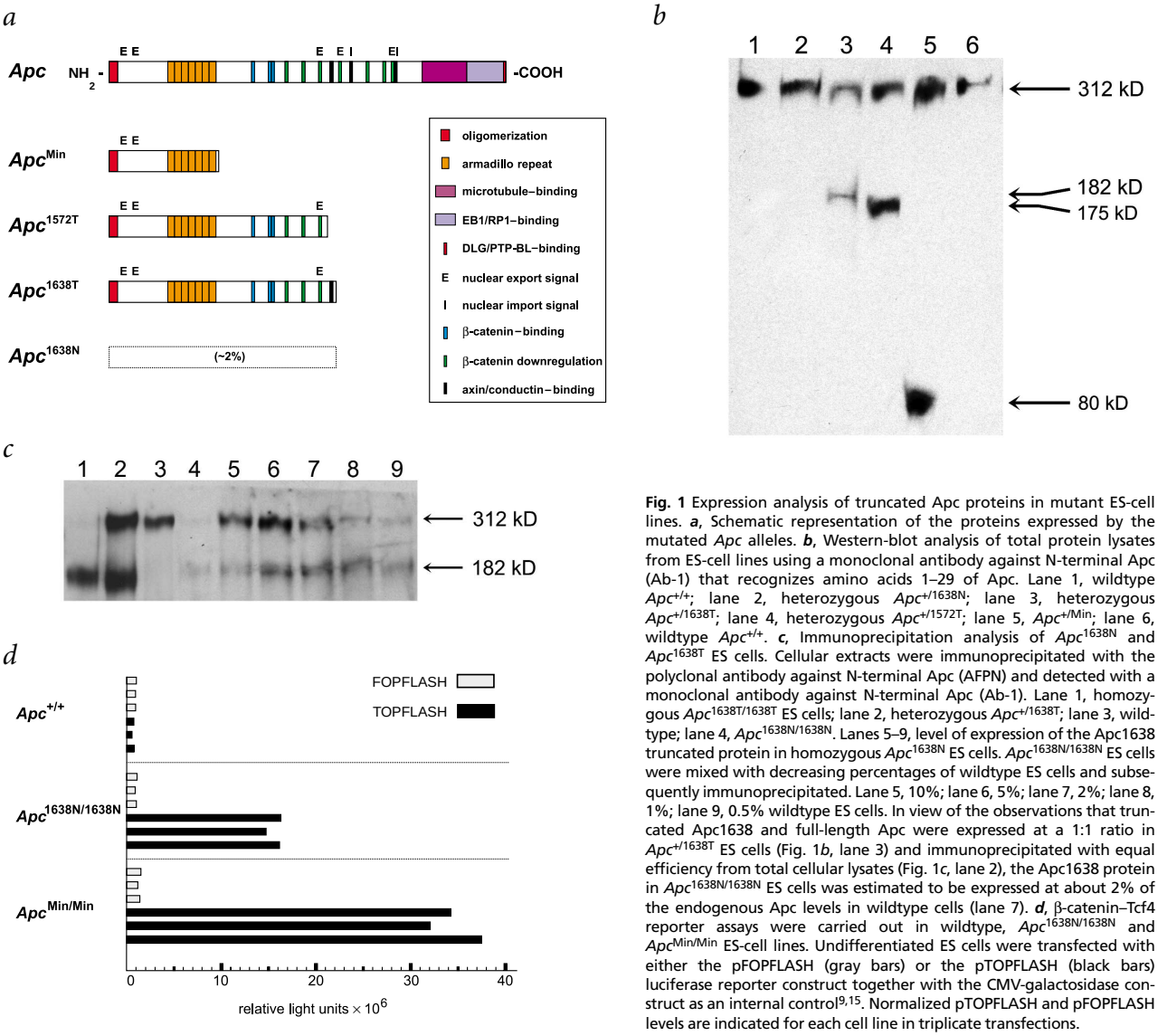

Fig. 1 Expression analysis of truncated Apc proteins in mutant ES-cell lines. ***a***, Schematic representation of the proteins expressed by the mutated *Apc* alleles. ***b***, Western-blot analysis of total protein lysates from ES-cell lines using a monoclonal antibody against N-terminal Apc (Ab-1) that recognizes amino acids 1–29 of Apc. Lane 1, wildtype $Apc^{+/+}$; lane 2, heterozygous $Apc^{+/1638N}$; lane 3, heterozygous $Apc^{+/1638T}$; lane 4, heterozygous $Apc^{+/1572T}$; lane 5, $Apc^{+/Min}$; lane 6, wildtype $Apc^{+/+}$. ***c***, Immunoprecipitation analysis of Apc^{1638N} and Apc^{1638T} ES cells. Cellular extracts were immunoprecipitated with the polyclonal antibody against N-terminal Apc (AFPN) and detected with a monoclonal antibody against N-terminal Apc (Ab-1). Lane 1, homozygous $Apc^{1638T/1638T}$ ES cells; lane 2, heterozygous $Apc^{+/1638T}$; lane 3, wildtype; lane 4, $Apc^{1638N/1638N}$. Lanes 5–9, level of expression of the Apc1638 truncated protein in homozygous Apc^{1638N} ES cells. $Apc^{1638N/1638N}$ ES cells were mixed with decreasing percentages of wildtype ES cells and subsequently immunoprecipitated. Lane 5, 10%; lane 6, 5%; lane 7, 2%; lane 8, 1%; lane 9, 0.5% wildtype ES cells. In view of the observations that truncated Apc1638 and full-length Apc were expressed at a 1:1 ratio in $Apc^{+/1638T}$ ES cells (Fig. 1*b*, lane 3) and immunoprecipitated with equal efficiency from total cellular lysates (Fig. 1*c*, lane 2), the Apc1638 protein in $Apc^{1638N/1638N}$ ES cells was estimated to be expressed at about 2% of the endogenous Apc levels in wildtype cells (lane 7). ***d***, β-catenin–Tcf4 reporter assays were carried out in wildtype, $Apc^{1638N/1638N}$ and $Apc^{Min/Min}$ ES-cell lines. Undifferentiated ES cells were transfected with either the pFOPFLASH (gray bars) or the pTOPFLASH (black bars) luciferase reporter construct together with the CMV-galactosidase construct as an internal control[9,15]. Normalized pTOPFLASH and pFOPFLASH levels are indicated for each cell line in triplicate transfections.

different genotypes. $Apc^{1638N/1638N}$ ES cells showed the highest reporter activity, followed by $Apc^{1638N/1572T}$, $Apc^{1638N/1638T}$ and $Apc^{1638T/1638T}$, the latter having reporter activity comparable to that of wildtype ES cells[9]. As the initial analysis did not include Apc^{Min}, we isolated both $Apc^{Min/Min}$ and $Apc^{1638N/1638N}$ ES-cell lines directly from blastocysts of mixed genetic background C57BL6/CD1. Although direct comparison between the former (using 129-Ola ES-cell lines) and the latter reporter assays is not feasible owing to the different genetic backgrounds, $Apc^{Min/Min}$ ES cells showed considerably higher (twofold) TOPFLASH reporter levels than did $Apc^{1638N/1638N}$ ES cells (Fig. 1*d*).

Hence, our collection of ES-cell lines with mutations in *Apc* show a gradient of β-catenin regulatory activity that may be useful in studying its dose-dependent consequences on different cellular functions.

In vivo differentiation analysis of ES-cell lines with mutations in *Apc* by teratoma formation

To evaluate the differentiation potential of the cell lines with mutations in *Apc* in an *in vivo* assay, we injected undifferentiated ES cells subcutaneously into syngenic mice to induce formation of teratomas. These are benign tumors derived from pluripotent stem cells and composed of well differentiated tissues of ecto-, meso- and endodermal origin[16]. Differentiation profiles of the resulting teratomas were investigated by histological and immunohistochemical analysis, and compared with those obtained with wildtype ($Apc^{+/+}$) ES cells (Fig. 2*a*).

Teratomas derived from independent $Apc^{1638N/1638N}$ ES-cell lines either obtained by two rounds of gene targeting or derived from blastocysts showed severe differentiation defects (Fig. 2*b*,*c*). Several differentiation types were absent, namely neural, bone, cartilage and ciliated epithelia. As neural differentiation is sometimes difficult to recognize using morphological criteria, we used four different neural markers to identify neuroectodermal cellular types, specifically neurons, astrocytes, Schwann cells (detected with neural cell adhesion molecule (NCAM) and glial fibrillary acidic protein (GFAP)), neurofilaments and synaptic vesicles. These antibodies did not stain homozygous Apc^{1638N} sections, in contrast with wildtype teratomas in which approximately 50–75% of the cells were positively stained (Fig. 2*g*–*j*,*l*–*o*). Differentiation to striated muscle (detected with adult myosin) was also severely affected and detectable in only a minority of the sections (data not shown). In contrast, smooth-muscle cellular types (detected with smooth muscle actin, 1A4) were abundant in Apc^{1638N} teratomas (Fig. 2*k*,*p*). Other cell types and tissues that we positively identified in the Apc^{1638N} teratomas included simple non-ciliated epithelia, keratinized epithelia and non-

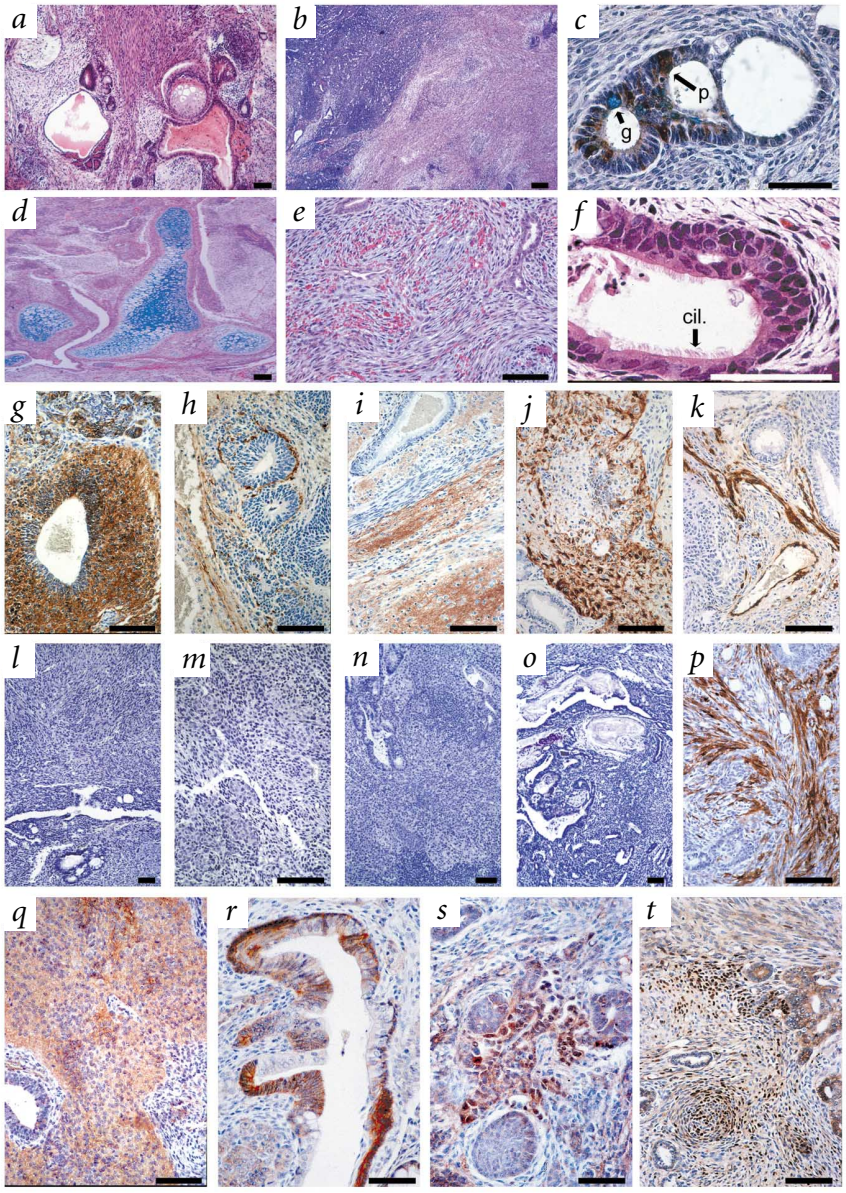

Fig. 2 *In vivo* differentiation analysis of teratomas derived from wildtype and mutant ES cells. Low-magnification view of histological sections stained with hematoxylin and eosin shows the heterogeneous differentiation profile of teratomas derived from wildtype ES cells (***a***) compared with the more homogeneous and undifferentiated histological features of teratomas derived from homozygous Apc^{1638N} ES cells (***b***). ***c***, Detail of homozygous Apc^{1638N} teratomas stained with an antibody against lysozyme identifying Paneth cells (p) within a non-ciliated secretory epithelium, and teratomas stained with Alcian blue identifying secretory goblet cells (g), both indicative of intestinal differentiation. ***d***, Histological section of a homozygous Apc^{1638T} teratoma stained with Alcian blue and hematoxylin shows cartilage/bone (blue) differentiation. Sections of compound heterozygous $Apc^{1638N/1572T}$ teratomas stained with hematoxylin and eosin showed a high degree of vascularization (***e***) and a ciliated secretory epithelium (cil; ***f***) that were absent in $Apc^{1638N/1638N}$ teratomas. Immunohistochemical staining of paraffin sections from wildtype (***g***–***k***) and homozygous $Apc^{1638N/1638N}$ (***l***–***p***) teratomas with neural markers NCAM (*g*,*l*), neurofilament (*h*,*m*), synaptic vesicles (*i*,*n*), GFAP (*j*,*o*) and smooth muscle (*k*,*p*). The slides were lightly counterstained with hematoxylin. ***q***–***t***, Expression and subcellular localization of β-catenin in teratomas derived from ES cells with mutations in *Apc*. Paraffin sections were stained for β-catenin by immunohistochemistry and counterstained with hematoxylin. *q*, Wildtype teratomas showed mainly cytoplasmic and membraneous β-catenin staining. *r*, $Apc^{1638N/1638T}$ teratomas showed a clear increase and heterogeneity of intracellular β-catenin. *s*, $Apc^{1638N/1572T}$ teratomas showed moderate nuclear β-catenin staining. *t*, $Apc^{1638N/1638N}$ teratomas showed strong nuclear β-catenin staining in cells undergoing mesenchymal condensation and epithelial differentiation. Scale bars = 0.1 mm.

Table 1 • Tissue-specific gene expression profiles in teratomas with mutations in *Apc*

Unigene	Gene symbol and name	Factor of difference relative to wildtype			
		$Apc^{1638N/1638N}$	$Apc^{1638N/1572T}$	$Apc^{1638N/1638T}$	$Apc^{1638T/1638T}$
Neural-specific genes					
Mm.1287	*Mapt** (microtubule-associated protein τ)	–100	–100	–2.3	1.1
Mm.1287	*Mapt** (microtubule-associated protein τ)	–95.5	–100	–2.6	–1.1
Mm.3304	*Nsg2* (neuron-specific gene family member 2)	–74.1	–64.6	–4.5	–1.5
Mm.4599	*Astn1* (astrotactin 1)	–53.7	–30.2	–3.4	–1.4
Mm.40615	*Kcnq2* (potassium voltage-gated channel subfamily Q member 2)	–52.5	–25.1	–5.1	–2.2
Mm.2496	*Ina* (α internexin neuronal intermediate filament protein)	–100	–69.2	–2.7	–1.1
Mm.1419	*Aqp4** (aquaporin 4)	–45.7	–20.4	–1.3	2.4
Mm.1419	*Aqp4** (aquaporin 4)	–18.2	–8.1	–1.4	2.2
Mm.34637	*Catna2** (catenin α 2)	–39.8	–36.3	–5.6	–1.7
Mm.34637	*Catna2** (catenin α 2)	–8.3	–3.5	–2.6	1.1
Mm.34637	*Catna2** (catenin α 2)	–6.8	–10.5	–2.4	–1
Mm.5309	*Gabrg2* (γ-aminobutyric acid A receptor subunit γ 2)	–37.2	–24.5	–4.7	–1.3
Mm.5101	***Syt1* (synaptotagmin 1)**	**–27.5**	**–14.5**	**–12.3**	**–12.3**
Mm.2991	*Oprl* (opioid receptor-like)	–18.2	–8.5	–7.4	–1.7
Mm.57194	*L1cam* (L1 cell adhesion molecule)	–18.2	–11.2	–8.3	–10.2
Mm.28562	***Syt9* (synaptotagmin 9)**	**–17.8**	**–17.8**	**–3**	**–1.2**
Mm.2419	*Cdh4* (cadherin 4)	–17.4	–6.6	–2.3	1
Mm.1239	***Gfap* (glial fibrillary acidic protein)**	**–13.8**	**–4.8**	**–1.7**	**2**
Mm.20892	***Syn2* (synapsin II)**	**–8.3**	**–5.8**	**–1.7**	**–1**
Mm.4974	***Ncam1* (neural cell adhesion molecule 1)**	**–7.6**	**–7.6**	**–2.5**	**–1.5**
Mm.4921	*Gria2* (glutamate receptor ionotropic AMPA2 α2)	–7.2	–23.4	–4.7	–1.5
Mm.180868	***Syt11* (synaptotagmin 11)**	**–6.6**	**–6.5**	**–3.3**	**–3.4**
Mm.4920	*Gria1* (glutamate receptor ionotropic AMPA1 α1)	–6.2	–10.7	–3.4	–1.5
Mm.10696	*Nrg1* (neuregulin 1)	–5	–1.2	–1.4	1.2
Bone- and cartilage-specific genes					
Mm.4987	*Ibsp* (integrin-binding sialoprotein)	–4.4	–19.1	–2	–1.4
Mm.4778	*Cspg3* (chondroitin sulfate proteoglycan 3)	–10	–4.4	–7.2	–3
Mm.2759	*Agc1* (aggrecan 1)	–4.4	–5.2	1.5	–2.9
Mm.5091	*Spock1* (sparc/osteonectin cwcv and kazal-like domains proteoglycan 1)	–2.3	–3.7	–2.5	–2
Mm.7964	*Cdrap* (cartilage-derived retinoic acid–sensitive protein)	–10.7	–3.8	–1.3	1
Muscle-specific genes					
Mm.1529	*Mylpc* (myosin light chain phosphorylatable cardiac ventricles)	–34.7	–16.2	2.9	1.1
Mm.46514	*Mylc2a* (myosin light chain regulatory A)	–13.2	–9.1	4.7	1.3
Mm.16528	***Myog* (myogenin)**	**–1.6**	**4.2**	**2.1**	**1.8**
Mm.3153	*Myh11* (myosin heavy chain 11 smooth muscle)	2.2	1.6	5.1	2.2
Mm.36850	***Smtn* (smoothelin)**	**19.1**	**13.5**	**9.5**	**–2.2**
Intestine-specific genes					
Mm.15621	*Cftr* (cystic fibrosis transmembrane conductance regulator homolog)	5.6	3.8	1.4	2.3
Mm.10805	*Col13a1* (procollagen type XIII α 1)	6.6	6.6	–1.1	1.5
Mm.4010	*Vil* (villin)	8.7	4.2	2.3	1.6
Mm.27830	*Slc7a8* (solute carrier family 7, cationic a a. transporter, y+ system, member 8)	12.3	2.8	–1.1	1.9
Mm.57132	*Defcr-ps1* (defensin-related cryptdin pseudogene 1)	16.6	4	–1.1	1.3
Mm.157909	*Defcr-rs1* (defensin-related sequence cryptdin peptide paneth cells)	32.4	7.2	1.2	1.3
Mm.140173	*Defcr5* (defensin-related cryptdin 5)	47.9	8.7	–1.3	2.7
Mm.14271	*Defcr-rs2* (defensin-related cryptdin related sequence 2)	60.3	4.4	3	1.8
Lung-specific genes					
Mm.7420	***Tubb4* (tubulin β 4)**	**–16.6**	**–47.9**	**–2.6**	**–1.1**
Mm.10414	*Mlf1* (myeloid leukemia factor 1)	–10	–4.6	–2.4	1.1
Mm.42257	*Tekt1* (tektin 1)	–6.8	–3.7	–2	1.3
Globin genes					
Mm.2308	*Hbb-bh1** (hemoglobin Z β-like embryonic chain)	4.9	11	4.7	3.2
Mm.2308	*Hbb-bh1** (hemoglobin Z β-like embryonic chain)	26.9	18.6	4.5	–1.7
Mm.141758	*Hba-x* (hemoglobin X α-like embryonic chain in Hba complex)	15.8	28.8	7.2	–1.1
Mm.35830	*Hbb-y* (hemoglobin Y β-like embryonic chain)	100	81.3	16.2	–1.3

Genes whose expression patterns were validated by immunohistochemistry are indicated in bold. The listed entries were selected based on their tissue-specific expression from the unsupervised agglomerative cluster analysis by the error model in Rosetta Resolver v3.0 Gene Expression Data Analysis System. A total of 1,484 genes were included that differed by a factor of 2 with $P < 0.01$ when compared with the wild type ($Apc^{+/+}$). Some genes (marked with an asterisk and listed next to each other in the table) have multiple independent entries in the Affymetrix microarray that we used. As expected, variations in the corresponding factor of difference were observed, although the general trend of differential expression was concordant.

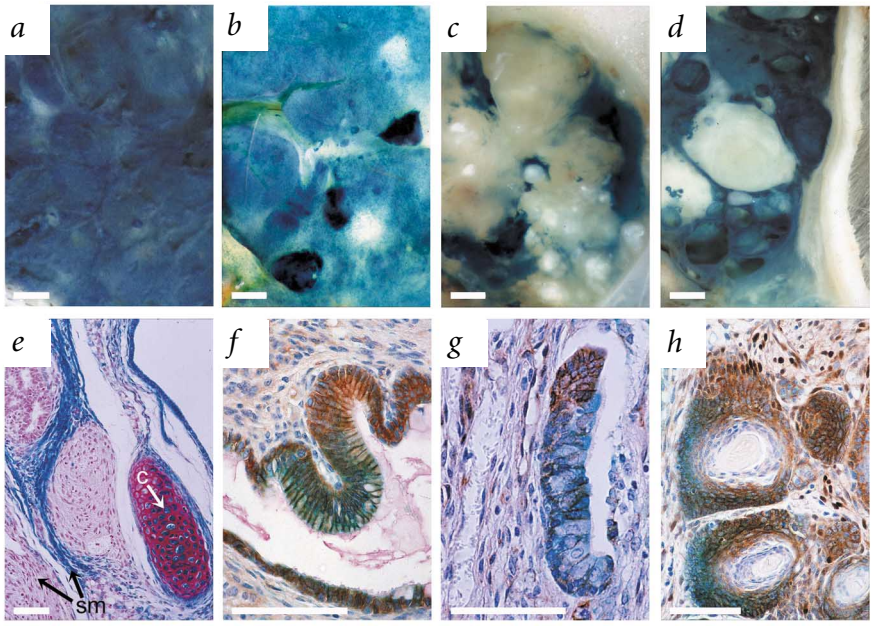

Fig. 3 Analysis of chimeric teratomas showed the cell-autonomous nature of the differentiation defect of ES cells with mutations in *Apc*. ***a***, Stereomicroscopic view of a wildtype *Apc* teratoma solely composed of ES cells targeted with a Rosa26-β-geo construct showing uniform lacZ expression (blue). ***b***, Stereomicroscopic view of a chimeric teratoma composed of wildtype Rosa26-β-geo (blue) and non-tagged (white) wildtype ES cells showing uniform amalgamation of the two cell types, resulting in a light blue appearance with small patches of unicellular contribution. ***c***, Stereomicroscopic view of a chimeric teratoma composed of tagged wildtype (blue) and $Apc^{1638N/1638N}$ (white) ES cells showing a non-uniform distribution of the two cell types. ***d***, Stereomicroscopic view of a chimeric teratoma composed of tagged wildtype (blue) and $Apc^{1638N/1572T}$ (white) ES cells showing the same sorting mechanism as in *c*. ***e***, Histological section of chimeric Rosa26-β-geo-$Apc^{+/+}$ (blue) and $Apc^{1638N/1638N}$ (red) ES cells stained for β-galactosidase activity (turquoise blue) and counterstained with basic fuchsin (red nuclei), showing contribution of both cell types in smooth muscle (sm) and of exclusively Rosa26-β-geo cells in cartilage (c). ***f–h***, Histological sections of chimeric Rosa26-β-geo-$Apc^{+/+}$/non-tagged $Apc^{+/+}$ ES teratomas (*f*) and of Rosa26-β-geo-$Apc^{+/+}$/non-tagged $Apc^{1638N/1638N}$ teratomas (*g* and *h*) stained for β-galactosidase activity (turquoise blue cytoplasm), immunostained against β-catenin (brown) and counterstained with hematoxylin (blue nuclei). β-catenin was homogeneously expressed in the chimeric epithelium composed of the same cell type (*f*). The mutant epithelium expressed high levels of β-catenin and had differentiated to non-ciliated epithelium (*g*, white arrowhead), whereas the wildtype part containing relatively low levels of β-catenin had differentiated to ciliated epithelium (*g*, black arrowhead). This nicely demonstrates the correlation between the *Apc* defect, increased β-catenin dose and differentiation. *h*, Nuclear translocation of β-catenin in mutant cells was not prevented by surrounding wildtype cells. White bar = 1 mm; black bar = 0.1 mm.

ciliated secretory epithelia including Paneth cells, which are indicative of intestinal differentiation (Fig. 2*c*). Hence, homozygous Apc^{1638N} ES cells showed severe differentiation defects that affected the neuroectodermal, dorsal mesodermal and endodermal lineages. In contrast, teratomas derived from homozygous $Apc^{1638T/1638T}$ or from compound $Apc^{1638N/1638T}$ ES cells were indistinguishable from wildtype teratomas at both the immunohistochemical and histological levels (Fig. 2*d* and data not shown), indicating that the differentiation defects observed in the $Apc^{1638N/1638N}$ teratomas were directly correlated to the quantitative expression of the 182-kD truncated protein.

We analyzed β-catenin expression in the teratomas by immunohistochemistry (Fig. 2*q–t*) and observed intense and abundant nuclear staining in the $Apc^{1638N/1638N}$ teratomas. The nuclear staining was not observed in every cell, but was clearly present in structures undergoing mesenchymal condensation and epithelial differentiation, a process known to be mediated by Wnt signaling[17] (Fig. 2*t*). Notably, compound heterozygous $Apc^{1638N/1638T}$ teratomas in which the Apc1638 protein was expressed at approximately 50% of the level observed in homozygous Apc^{1638T} cells did not show clear nuclear β-catenin accumulation but showed differences in β-catenin cytoplasmic staining patterns between flanking epithelial sheets, suggesting a more subtle defect of its downregulation by Apc (Fig. 2*r*). These abnormal staining patterns were never observed in $Apc^{1638T/1638T}$ or wildtype teratomas. The low dose (2%) of the Apc1638 protein in homozygous Apc^{1638N} teratomas seemed, therefore, to be insufficient to prevent nuclear accumulation of β-catenin during differentiation. On the other hand, a 50% increase in the dose of this truncated protein, as expressed by the $Apc^{1638N/1638T}$ teratomas, was sufficient to prevent β-catenin nuclear accumulation.

These results point to a direct relationship between nuclear accumulation of β-catenin and differentiation. To test this hypothesis, we analyzed the differentiation potential of Apc1572T, a truncated Apc protein almost identical to Apc1638T except for the deletion of the last residual SAMP repeat (axin-binding domain; ref. 9; Fig. 1*a*). The Apc1572T protein was stably expressed (Fig. 1*b*), but its ability to downregulate β-catenin was impaired owing to its failure to bind axin. The Apc^{1572T} mutation was targeted in ES cells in both the heterozygous ($Apc^{+/1572T}$) and compound $Apc^{1638N/1572T}$ forms to allow comparison with $Apc^{1638N/1638T}$ and $Apc^{1638N/1638N}$ cells. Teratomas derived from $Apc^{+/1572T}$ ES cells had normal differentiation profiles whereas those derived from compound heterozygous $Apc^{1638N/1572T}$ ES cells had much lower differentiation potential than $Apc^{1638N/1638T}$ and wildtype counterparts. The differentiation defects of $Apc^{1638N/1572T}$ ES cells closely resembled those observed in $Apc^{1638N/1638N}$ teratomas, except that they maintained their capacity to differentiate into ciliated epithelia (Fig. 2*e*,*f*). Nuclear translocation of β-catenin was also evident, although the frequency and intensity were somewhat lower than those observed in the homozygous Apc^{1638N} teratomas (Fig. 2*s*). Thus, removal of the only axin-binding motif in the Apc1638T protein resulted in nuclear translocation of β-catenin and in considerably lower differentiation potential.

Expression profiling of teratomas with mutations in *Apc* by oligonucleotide microarrays

The differentiation defect that we observed in teratomas with mutations in *Apc* by immunohistochemical analysis probably resulted from profound changes in gene expression patterns. We analyzed the teratomas by oligonucleotide microarrays encompassing probes for approximately 12,000 mouse genes and expressed sequence tags. Poly(A)$^+$ RNA was isolated from teratomas derived from wildtype ($Apc^{+/+}$), $Apc^{1638N/1638N}$, $Apc^{1638N/1638T}$, $Apc^{1638N/1572T}$ and $Apc^{1638T/1638T}$ ES-cell lines and hybridized to the oligonucleotide microarrays. We used the gene expression profiles from the mutant teratomas to select for tissue-specific genes that were up- or downregulated relative to wildtype tumors.

We observed a strong correlation between the morphological and immunohistochemical characterization of the mutant teratomas and their tissue-specific expression profiles (Table 1). In particular, a large collection of neuroectodermal-specific probes were shown to be consistently downregulated among the teratomas with mutations in *Apc* (Table 1), in agreement with previous histological and immunohistochemical observations (Fig. 2). Mesoderm-derived lineages such as bone and cartilage were also absent in mutant teratomas. Accordingly, bone- and cartilage-specific genes were considerably downregulated (Table 1). Other mesodermal lineages such as smooth and striated muscle were present and absent, respectively, in the mutant teratomas, as also shown by the differential up- and downregulation of the specific gene markers (Table 1). Specific endodermal lineages were also differentially represented in mutant teratomas: whereas non-ciliated epithelia of intestinal type were present (Fig. 2), ciliated epithelia such as those of the respiratory tract were under-represented or absent. Microarray analysis confirmed the upregulation of several intestinal markers (for example, defensin-related cryptdins), whereas lung-specific genes were downregulated (Table 1). Notably, we observed upregulation by a factor of up to 100 of embryonic α- and β-like globin genes in the mutant tissues (Table 1).

The *Apc* differentiation defect is cell-autonomous

To investigate the cellular nature of the differentiation defect that results from loss of Apc function, we generated chimeric teratomas composed of either $Apc^{1638N/1638N}$ or $Apc^{1638N/1572T}$ cells mixed with $Apc^{+/+}$ ES cells, the latter tagged with a constitutively expressed β-galactosidase gene (Rosa26-β-geo)[18]. We generated chimeric teratomas with wildtype ES cells mixed with their Rosa26-β-geo–targeted counterpart. This resulted in a homogeneous mixture of blue and unstained cells with a light blue macroscopic appearance when compared with teratomas made exclusively of wildtype Rosa26-β-geo ES cells (Fig. 3*a*,*b*). When wildtype Rosa26-β-geo ES cells were used together with ES cells with mutations in *Apc* to generate teratomas, we found all differentiated cell lineages in the resulting chimeric tumors, indicating that the homozygous Apc^{1638N} and compound $Apc^{1638N/1572T}$ ES cells did not affect the differentiation potential of wildtype ES cells (Fig. 3).

In chimeric teratomas, the wildtype cells differentiated into tissues otherwise never observed in teratomas derived from $Apc^{1638N/1638N}$ and $Apc^{1638N/1572T}$ cells only, whereas other tissues contained both mutant and wildtype cells, showing that the *Apc* differentiation defect is cell-autonomous. Accordingly, β-catenin staining was markedly elevated and often nuclear in homozygous Apc^{1638N} cells, but was cytoplasmic and membrane-bound in wildtype cells, even in chimeric epithelia where mutant and wildtype cells were in direct contact with each other (Fig. 3*e*–*h*). Thus, the *Apc* mutation is cell-autonomous with respect to both differentiation and β-catenin downregulation capacity.

Notably, we observed cell sorting when we analyzed the chimeric teratomas macroscopically (Fig. 3*c*,*d*). We observed this non-uniform distribution of wildtype and mutant cells with both the homozygous Apc^{1638N} and compound $Apc^{1638N/1572T}$ ES-cell lines. The cell sorting was probably due to homotypic cell–cell recognition. Further studies will elucidate the molecular and cellular mechanisms underlying this phenomenon.

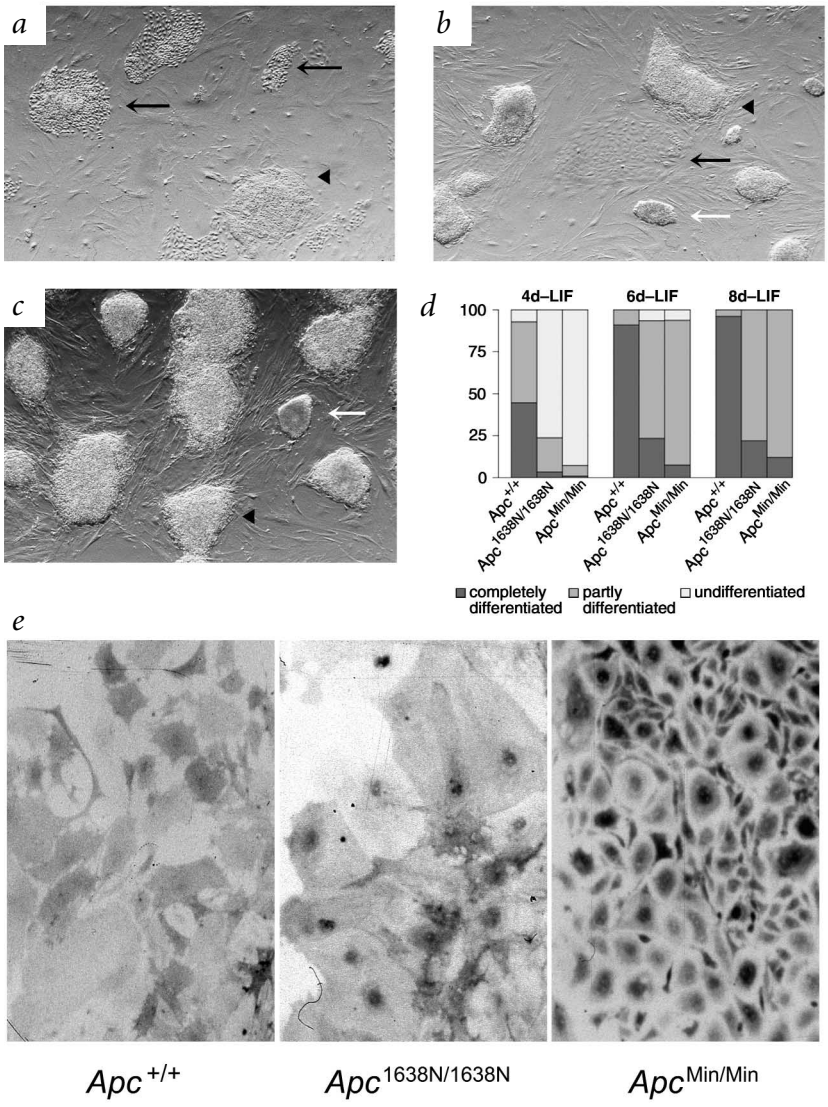

Fig. 4 *In vitro* differentiation analysis of Apc^{Min} and Apc^{1638N} ES cells. Wildtype (***a***), homozygous $Apc^{1638N/1638N}$ (***b***) and $Apc^{Min/Min}$ (***c***) ES cells were cultured for 2 d with LIF. LIF was then withdrawn so that differentiation could occur, and colonies were monitored at 4, 6 and 8 d after the start of the cultures. Data shown is from 8 d of culture. The colonies were subdivided in three categories: completely undifferentiated with no mesenchymal cells protruding from the edge of the ES colony (white arrows); partly differentiated with mesenchymal cells surrounding a core of undifferentiated cells (black arrowheads); and completely differentiated, composed exclusively of mesenchymal cells (black arrows). ***d***, Number (percentage of total) of completely undifferentiated (white bars), partly differentiated (gray bars) and completely differentiated (black bars) wildtype and mutant ES colonies after 4, 6 and 8 d of culture in absence of LIF. The value for each bar was determined from counting over 200 colonies from independently cultured plates and randomly selected stereomicroscopic fields. Results were confirmed by two independent experiments. ***e***, β-catenin immunohistochemical staining of colonies differentiated *in vitro* showed absent, moderate and strong β-catenin nuclear accumulation in wildtype, $Apc^{1638N/1638N}$ and $Apc^{Min/Min}$ ES cells, respectively.

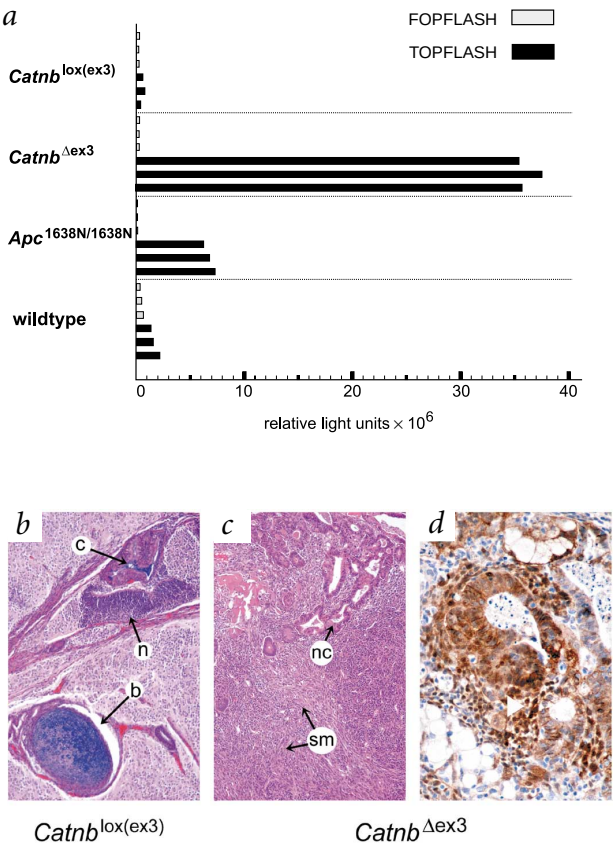

Fig. 5 Biochemical and immunohistochemical analysis of teratomas with mutations in *Catnb*. ***a***, β-catenin–Tcf reporter assays were carried out in wildtype (*Apc*$^{+/+}$ *Catnb*$^{+/+}$), *Apc*$^{1638N/1638N}$ *Catnb*$^{lox(ex3)}$ (equivalent to wildtype) and *Catnb*$^{\Delta ex3}$ (mutated) ES-cell lines. Undifferentiated ES cells were transfected with either the pTOPFLASH (black bars) or the pFOPFLASH (gray bars) luciferase reporter construct, together with the *R. reniformis* luciferase construct as an internal control[9,15]. Normalized pTOPFLASH and pFOPFLASH levels are indicated for each cell line from triplicate transfections. ***b,c***, Differentiation profiles of teratomas with mutations in *Catnb*. Hematoxylin and eosin staining of paraffin-embedded sections of teratomas derived from generated *Catnb*$^{lox(ex3)}$ (*b*) and *Catbn*$^{\Delta ex3}$ (*c*) ES cells. ***d***, Expression and subcellular distribution of β-catenin in teratomas derived from *Catbn*$^{\Delta ex3}$ ES cells. Paraffin sections were stained for β-catenin by immunohistochemistry and counterstained with hematoxylin. Overexpression and nuclear localization of β-catenin was observed in mesenchymal cell types (white arrowhead), among others. c, ciliated epithelium; n, neural lineages; b, bone; nc, non-ciliated epithelium; sm, smooth muscle.

Apc$^{Min/Min}$ ES cells did not form teratomas

The above results are indicative of a dose-dependent defect in Apc in ES-cell differentiation, possibly owing to partial loss of β-catenin regulation. The *Apc*^{Min} allele encodes a short truncated protein lacking all the β-catenin binding and downregulating domains and, therefore, is unable to control Wnt/β-catenin signaling. We attempted teratoma formation using independent blastocyst-derived *Apc*$^{Min/Min}$ ES-cell lines together with ES-cell lines derived from *Apc*$^{+/+}$ and *Apc*$^{+/Min}$ littermates as controls. Notably, all attempts to generate teratomas with *Apc*$^{Min/Min}$ ES-cell lines failed in our *in vivo* assay, whereas their *Apc*$^{+/+}$ and *Apc*$^{+/Min}$ counterparts gave rise to teratomas with normal differentiation patterns.

In vitro differentiation analysis of *Apc*$^{Min/Min}$ and *Apc*$^{1638N/1638N}$ ES cells

The inability of *Apc*$^{Min/Min}$ ES-cell lines to form teratomas indicates a severe differentiation defect that may be due to the complete loss of β-catenin downregulating activity in this allele. To study in more detail the cellular nature of the most severe *Apc* differentiation defects, we carried out *in vitro* differentiation analysis of *Apc*$^{Min/Min}$ and *Apc*$^{1638N/1638N}$ ES-cell lines by simply withdrawing leukemia inhibiting factor (LIF) from the culture medium and by analyzing cell morphology at different time intervals when compared with wildtype cells (Fig. 4). In general, *Apc*$^{Min/Min}$ and *Apc*$^{1638N/1638N}$ ES cells differentiated at a much lower rate than their wildtype counterparts (eight days and two days, respectively). Although we eventually observed differentiation in both *Apc*$^{Min/Min}$ and *Apc*$^{1638N/1638N}$ ES cells, they seemed to maintain their undifferentiated state in culture for a considerably longer period than wildtype and heterozygous controls.

To identify the cell types formed after differentiation, we analyzed ES-cell colonies by immunohistochemical staining with different lineage-specific antibodies. Similar to teratomas, *Apc*$^{1638N/1638N}$ colonies formed massive amounts of smooth muscle but did not form neuroectodermal derivatives. *Apc*$^{Min/Min}$ colonies formed large amounts of visceral and parietal endoderm (identified by morphology and by antibodies against α-fetoprotein and vimentin, respectively) but did not differentiate into smooth muscle cells or nerve cells. Notably, after prolonged culture of *Apc*^{Min} cells, only extensive epithelial sheets of parietal endoderm were present (data not shown).

Next, we tried to modulate *in vitro* differentiation of the *Apc*^{Min} and *Apc*^{1638N} ES cells towards neuroectodermal, mesodermal and trophectodermal lineages by complementing the culture medium with retinoic acid, dimethyl sulfoxide and fibroblast growth factor 4, respectively[19,20]. Compared with the wildtype ES-cell line, neither *Apc*$^{Min/Min}$ nor *Apc*$^{1638N/1638N}$ ES cells responded to these stimuli, as we observed no change in their morphology or expression of tissue-specific markers (data not shown). This indicates that the differentiation defects cannot be rescued by external factors.

We also stained *Apc*^{Min} and *Apc*^{1638N} ES clones differentiated *in vitro* for β-catenin and compared them to *Apc*$^{+/+}$ ES cells (Fig. 4*e*). An intense nuclear signal was present in most *Apc*$^{Min/Min}$ cells. *Apc*$^{1638N/1638N}$ cells also had nuclear β-catenin, although the signal intensity was considerably weaker and less abundant than in the *Apc*^{Min} clones. Wildtype ES cells did not show any nuclear accumulation of β-catenin. Excessive β-catenin accumulation in the nucleus has been shown to result in programmed cell death[21], which may explain the inability of *Apc*$^{Min/Min}$ to form teratomas.

Impaired differentiation in ES cells with mutations in *Catnb*

We confirmed that the differentiation defect observed in ES cells with mutations in *Apc* was due to the loss of the β-catenin regulating function by repeating the teratoma differentiation assay with ES cells carrying a Cre–*lox*P mediated deletion of exon 3 of β-catenin (ref. 22). This exon encompasses all serine/threonine residues of β-catenin, which are phosphorylation targets that earmark β-catenin for ubiquitination and proteolytic degradation. We used two ES-cell lines: *Catnb*$^{lox(ex3)}$, in which exon 3 of the β-catenin gene is flanked by *lox*P sites without compromising functionality of the corresponding allele, and *Catnb*^{ex3}, which was obtained by Cre-mediated deletion of exon 3 (ref. 22). The two ES-cell lines were first analyzed by TOPFLASH reporter assay and compared with wildtype and *Apc*$^{1638N/1638N}$ ES-cell lines (Fig. 5*a*). *Catnb*^{ex3} ES cells had approximately three times higher reporter levels than did *Apc*$^{1638N/1638N}$ ES cells. Direct comparison between *Catnb*^{ex3} and *Apc*$^{Min/Min}$ ES cells was not feasible, as these lines were only available in different genetic backgrounds. TOPFLASH reporter levels in *Catnb*$^{lox(ex3)}$ were indistinguishable from those observed in wildtype cells.

Next, *Catnb*$^{lox(ex3)}$ and *Catnb*^{ex3} ES cells were assayed for their differentiation potential by teratoma formation. Teratomas were successfully derived from both cell lines. *Catnb*$^{lox(ex3)}$ differentiation profiles were indistinguishable from those obtained with wildtype ES cells, whereas *Catnb*^{ex3} cells formed teratomas with limited differentiation patterns, similar to those observed in *Apc*$^{1638N/1638N}$. In particular, ectoderm-derived cell lineages were absent, whereas an abundance of smooth muscle and non-ciliated epithelia was observed (Fig. 5*b*). Nuclear β-catenin localization (Fig. 5*b*) and other immunohistochemical observations obtained with the same set of antibodies that we used to analyze teratomas with mutations in *Apc* (data not shown) confirmed these aberrant differentiation patterns in the *Catnb*^{ex3} teratomas.

These data confirm that the differentiation defect observed in ES cells with mutations in *Apc* was due to improper β-catenin regulation. Moreover, different doses of residual β-catenin directly correlated with differences in differentiation potential and with the intensity and frequency of nuclear accumulation of β-catenin. Taken together, the data point to a dose-response effect between *Apc* mutations affecting the β-catenin downregulating function, the increase in β-catenin–mediated transcriptional activity and the differentiation defects in ES cells.

Expression profiling and data mining

Loss of β-catenin regulation may cause multiple changes in the transcription of several genes downstream in the Wnt pathway. To investigate the changes in gene expression that accompany the differentiation of wildtype and *Apc*-mutated ES cells, and to pinpoint potential key regulatory genes, we analyzed the teratomas with mutations in *Apc* by Affymetrix microarray technology. We compared expression data from the mutant teratomas with the wildtype tumors by an unsupervised, hierarchical clustering algorithm. This analysis correctly clustered the mutant teratomas characterized by aberrant differentiation (*Apc*$^{1638N/1638N}$ and *Apc*$^{1638N/1572T}$) apart from those that were indistinguishable from the wildtype tumors at the immunohistochemical level (*Apc*$^{1638N/1638T}$ and *Apc*$^{1638T/1638T}$; Fig. 6*a*). The majority of genes up- or downregulated in *Apc*$^{1638N/1638N}$, *Apc*$^{1638N/1572T}$

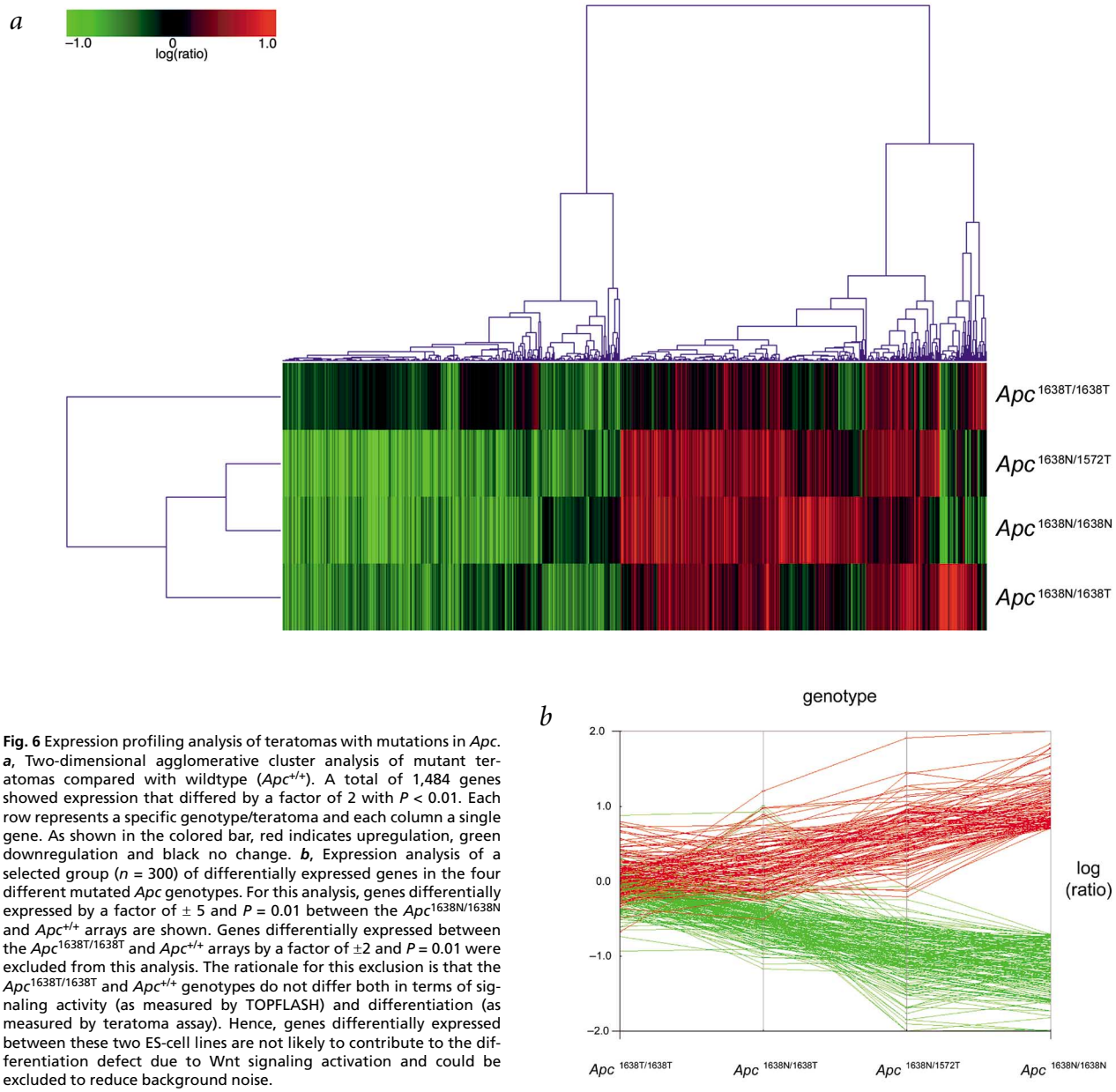

Fig. 6 Expression profiling analysis of teratomas with mutations in *Apc*. ***a***, Two-dimensional agglomerative cluster analysis of mutant teratomas compared with wildtype (*Apc*$^{+/+}$). A total of 1,484 genes showed expression that differed by a factor of 2 with $P < 0.01$. Each row represents a specific genotype/teratoma and each column a single gene. As shown in the colored bar, red indicates upregulation, green downregulation and black no change. ***b***, Expression analysis of a selected group ($n = 300$) of differentially expressed genes in the four different mutated *Apc* genotypes. For this analysis, genes differentially expressed by a factor of ± 5 and $P = 0.01$ between the *Apc*$^{1638N/1638N}$ and *Apc*$^{+/+}$ arrays are shown. Genes differentially expressed between the *Apc*$^{1638T/1638T}$ and *Apc*$^{+/+}$ arrays by a factor of ±2 and $P = 0.01$ were excluded from this analysis. The rationale for this exclusion is that the *Apc*$^{1638T/1638T}$ and *Apc*$^{+/+}$ genotypes do not differ both in terms of signaling activity (as measured by TOPFLASH) and differentiation (as measured by teratoma assay). Hence, genes differentially expressed between these two ES-cell lines are not likely to contribute to the differentiation defect due to Wnt signaling activation and could be excluded to reduce background noise.

and, to a lesser extent, $Apc^{1638N/1638T}$ teratomas were, in general, not changed in $Apc^{1638T/1638T}$ teratomas (Fig. 6*a*). This confirms that the mutated *Apc* genotypes that result in constitutive activation of Wnt signaling are characterized by distinct gene expression profiles when compared with teratomas derived from Wnt-proficient ES-cell lines (as judged by TOPFLASH reporter assays).

Among the differentially expressed entries, both structural tissue–specific (Table 1) and regulatory (Table 2) genes were identified. The latter belong to well-known signal-transduction pathways such as Wnt, transforming growth factor β, fibroblast growth factor and retinoic acid (Table 2). Although the elucidation of the signal-transduction pathways underlying the stem-cell differentiation caused by mutations in *Apc* is beyond the scope of the present study, the pattern of differential expression among these genes seems to agree with the differentiation defects observed in the mutant teratomas. For example, the upregulation of the bone morphogenetic proteins 2 and 4 (encoded by *Bmp2* and *Bmp4*; Table 2) may explain some of the observed differentiation defects. Bmp proteins are morphogenetic signaling proteins belonging to the Tgfβ superfamily originally isolated for their capacity to induce ectopic bone formation[23,24]. Bmp proteins signal through heteromeric complexes of type I and type II transmembrane Ser/Thr kinase receptors, triggering the expression of downstream target genes. Among the latter, the homeobox genes *Msx1* and *Msx2* have been previously reported to be induced by *Bmp2* and *Bmp4* (ref. 25) and are accordingly upregulated in teratomas with mutations in *Apc* (Table 2). Expression of *Msx1* (and *Msx2)* is known to interfere with the differentiation process by blocking cell-cycle exit through upregulation of cyclin D1 (ref. 26). Though the gene encoding cyclin D1 was not upregulated in our data set, the homolog cyclin D3 was (Table 2). The gene T-box 2 (*Tbx2*), a known modulator (both activator and repressor) of bone development whose activity largely depends on the cellular context, was also upregulated in teratomas with mutations in *Apc*[27] (Table 2). *Tbx2* expression is induced by *Bmp2* (ref. 28).

Table 2 • Signal-transduction gene expression profiles in teratomas with mutations in *Apc*.

Unigene	Gene symbol and name	Factor of difference relative to wildtype			
		$Apc^{1638N/1638N}$	$Apc^{1638N/1572T}$	$Apc^{1638N/1638T}$	$Apc^{1638T/1638T}$
Wnt pathway genes					
Mm.20355	*Wnt4* (wingless-related MMTV integration site 4)	18.6	3.9	5.6	5.2
Mm.22182	*Wnt11* (wingless-related MMTV integration site 11)	10.5	5.4 1	9 1	1
Mm.2438	*Wnt6* (wingless-related MMTV integration site 6)	8.1	1.9	–1.3	1.4
Mm.32207	*Wnt5a* (wingless-related MMTV integration site 5A)	7.1	3.2	–1 1	1
Mm.5130	*Wnt10a* (wingless-related MMTV integration site 10a)	6	1.3	1	1.9
Mm.45050	*Fzd1* (frizzled homolog 1 *Drosophila*)	3.3	1.7	–2.2	–3.9
Mm.103593	*Dkk2* (dickkopf 2)	21.9	14.1	1.9	–1.3
Mm.7960	*Dkk1* (dickkopf homolog 1 *Xenopus laevis*)	11.5	8.3	3.7	1.4
Mm.2029	*Lef1* (lymphoid enhancer binding factor 1)	2	1.3	–1.8	1.1
Mm.5080	*Sox17* (SRY-box containing gene 17)	4.8	4.2	3.5	1.9
Mm.2580	*Sdc1* (syndecan 1)	18.6	6.5	2.2	–1.1
Mm.4272	*Snai2* (snail homolog 2 *Drosophila*)	6.8	5 2	2 1	2
Mm.6813	*Bmp4** (bone morphogenetic protein 4)	3.9	2.3	1.4	–1.1
Mm.13828	*Wisp2* (WNT1 inducible signaling pathway protein 2)	5.1	2.8	1.9	1.5
Mm.7417	*Ccnd3* (cyclin D3)	2.6	3.2	2.1	–1.2
Mm.16234	*Itga5* (integrin α 5 fibronectin receptor α)	10 6	5	4.8	2.3
Mm.5039	*Six2* (sine oculis-related homeobox 2 homolog *Drosophila*)	7.9	8.7	1.9	–1.3
Tgfβ pathway genes					
Mm.57216	*Bmp2* (bone morphogenetic protein 2)	13	2 3	1.9	–1.2
Mm.6813	*Bmp4** (bone morphogenetic protein 4)	6.3	4.3	1.4	–1.4
Mm.9154	*Tgfb1* (transforming growth factor β 1)	5.5	2.8	–1.6	–3
Mm.18213	*Tgfb2* (transforming growth factor β 2)	4.1	2.4	–1.5	–1.4
Mm.8042	*Inhba* (inhibin β-A)	7.8	1.4	–1.7	1.2
Mm.9404	*Nbl1* (neuroblastoma suppression of tumorigenicity 1)	6 2	6 1	3	2.5
Mm.19307	*Ltbp1* (latent transforming growth factor β binding protein 1)	6 1	9 2	2	1.3
Mm.1763	*Msx2* (homeo box msh-like 2)	69.2	8.5	2.8	2.3
Mm.870	*Msx1* (homeo box msh-like 1)	5 3	2	–1.1	1.1
Mm.5194	*Dlx3* (distal-less homeobox 3)	17	4.1	1.4	–1.5
Mm.23467	*D5Ertd189e* (DNA segment Chr 5 ERATO Doi 189 expressed)	11.2	8.9	1.3	1.4
Mm.4605	*Tbx2* (T-box 2)	4.8	4.6	1.3	1.6
Mm.4509	*Runx2* (runt-related transcription factor 2)	8.7	2.6	–1	–1.8
Fgf pathway genes					
Mm.4912	*Fgfr4* (fibroblast growth factor receptor 4)	13.8	3.2	–1.3	–1.5
Mm.16340	*Fgfr2** (fibroblast growth factor receptor 2)	3.5	1.7	1	–6
Mm.3157	*Fgfr1* (fibroblast growth factor receptor 1)	3.2	1.9	1.2	1.3
Mm.16340	*Fgfr2** (fibroblast growth factor receptor 2)	2.5	1	–1	–2.5
Mm.2580	*Sdc1* (syndecan 1)	18.6	6.5	2.2	–1.1
Mm.67919	*Mafb* (v-maf musculoaponeurotic fibrosarcoma oncogene family protein B)	11.5	2.3	1.7	1.1
Retinoic acid pathway genes					
Mm.1273	*Rarg* (retinoic acid receptor γ)	46.8	10.7	2.8	–2
Mm.34797	*Crabp1* (cellular retinoic acid–binding protein I)	9.8	6.6	3.3	5.4
Mm.4757	*Crabp2* (cellular retinoic acid–binding protein II)	3.2	3.3	1.4	1.9

The listed entries were derived from the unsupervised agglomerative cluster analysis by the error model in Rosetta Resolver v3.0 Gene Expression Data Analysis System (1,484 genes included that differed by a factor of 2 with $P < 0.01$ when compared with the wild type ($Apc^{+/+}$)) and classified into the different signaling pathways based on the information provided by the Affymetrix Gene Ontology annotations. Some genes (marked with an asterisk) have multiple entries in the Affymetrix microarrays that we used.

Notably, we also found that dickkopf genes (*Dkk1* and *Dkk2*) were upregulated in teratomas with mutations in *Apc* (Table 2). *Dkk1* and *Dkk2* encode secreted proteins that act as potent inhibitors of Wnt signaling, are involved in head induction in *Xenopus laevis* embryogenesis and are highly expressed during mouse development in mesodermal tissues that mediate epithelial–mesenchyme transitions[29]. The upregulation of the *Dkk1* and *Dkk2* inhibitors is in apparent contradiction to the similar behavior of several Wnt-related genes, including inducers/ligands (Wnt-ligands), receptors (frizzled), transcription factors (lymphoid enhancer binding factor 1) and downstream targets (WNT1-inducible signaling pathway proteins, cyclins and others; Table 2). The complexity and tissue heterogeneity of the teratomas are confounding factors, however, as we cannot ascertain which tissues contribute to which differential gene expression patterns.

To visualize the Apc–β-catenin dose-dependent control of gene expression, we selected a subset of 300 highly differentially expressed genes in $Apc^{1638N/1638N}$ teratomas (that is, those that differed by a factor of >5 or <–5). We subtracted those that were differentially expressed in $Apc^{1638T/1638T}$ relative to wildtype teratomas (those that differed by a factor of >2 or <–2) and followed their behavior in the four genotypes (Fig. 6*b*). We observed a clear gradient of transcriptional response starting from the Wnt-proficient alleles ($Apc^{1638T/1638T}$) and gradually increasing (or decreasing) in more severely affected genotypes ($Apc^{1638N/1638T}$, $Apc^{1638N/1572T}$, $Apc^{1638N/1638N}$). This clearly indicates that different doses of β-catenin made available for Wnt signaling by specific *Apc* defects resulted in different target-gene expression responses and, consequently, in different degrees of ES-cell differentiation.

The rationale for our data mining approach (Fig. 6*b*) was the observation that the $Apc^{1638T/1638T}$ ES cells were shown to be Wnt- and differentiation-proficient by TOPFLASH reporter and by teratoma assays, respectively[9]. Hence, the differential expression in $Apc^{1638T/1638T}$ relative to wildtype teratomas was probably caused by β-catenin–independent effects. The recently characterized chromosomal instability of the ES-cell lines with mutations in *Apc* that we used[30] may partly account for this differential gene expression. Loss of this function of Apc in mitosis cannot possibly account for the differentiation defects reported here, however, as $Apc^{1638T/1638T}$ ES cells were shown to be chromosomally unstable but differentiation-proficient.

Discussion

In this study, we show that mutations in *Apc* affect the differentiation capacity of mouse ES cells in a quantitative and qualitative fashion depending on the dose of β-catenin signaling. This direct correlation between differentiation and Apc/β-catenin signal transduction has implications for understanding the cellular mechanism underlying *Apc*-driven tumorigenesis. Although it is generally accepted that the tumor-suppressor function of Apc resides in its ability to downregulate β-catenin[9,15,31–33], the tissue-specific downstream targets responsible for the broad tumor spectrum observed both in individuals affected with FAP[12] and *Apc*-mutated mouse models[6] are still largely unknown.

Our results are in agreement with the role of β-catenin signaling in maintaining stem-cell properties in the intestine, as also illustrated by the inability of mice that lack Tcf4 to form crypt stem cells[13]. In these mice, the neonatal epithelium is composed entirely of differentiated cells. Thus, the genetic program controlled by β-catenin signaling and executed by Tcf4 maintains the crypt stem cells of the small intestine and, on the basis of the data presented here, modulates differentiation. In the colonic epithelium, mitotic cell rates equal terminal differentiation and cell loss rates. Intestinal tumors are the result of an increase in this gain:loss ratio. In view of the present data, this increase may be the consequence of a differentiation defect resulting from the constitutive activation of β-catenin signaling by mutations in *Apc*. This may retard or inhibit differentiation and ultimately result in an enlargement of the stem-cell compartment, the target cell population that undergoes additional mutations eventually leading to tumor formation.

In an alternative but analogous scenario, a differentiated colonic epithelial cell undergoes *Apc* (or *Catnb*) mutation, thus triggering a process of de-differentiation and, again, enlargement of the stem-cell compartment within the crypt. This would agree with the recently postulated 'top-down' model of colorectal tumorigenesis in which neoplastic transformation is initiated in a fully differentiated cell that becomes dysplastic, spreads laterally and progressively replaces the normal crypt cells[34]. In general, colorectal tumors do show a high proportion of undifferentiated crypt-like cells with high numbers of dividing cells, although all differentiated cell types are still present[22,35]. The same correlation between activation of Wnt/β-catenin signaling and stem-cell maintenance may also apply to other tumor types, as it represents an effective way to sustain tumor growth in a broad spectrum of self-renewing tissues. Accordingly, a large number of tumor types are characterized by β-catenin overexpression and/or nuclear localization. Recently, it was shown that overexpression of *Pin1* is responsible for the frequently observed β-catenin upregulation in breast cancer, a tumor type in which mutations in *APC* or *CATNB* are not common[36]. Different mutation types in different members of the Wnt pathway will result in different signaling doses associated with specific tumors in susceptible tissues.

In conclusion, we report that mutations in *Apc* and *Catnb* affect the capacity of embryonic stem cells to differentiate into the three germ layers in a β-catenin dose-dependent fashion. These results have implications for understanding the molecular and cellular basis of tumor initiation by defects in the Wnt pathway. We propose a model in which adult somatic stem-cell compartments are characterized by tissue-specific β-catenin threshold levels for cell proliferation, differentiation and apoptosis. Different mutations in *Apc* will result in different levels of intracellular β-catenin and will confer different degrees of tumor susceptibility in different tissues. Hence, β-catenin dose-dependent differentiation may explain not only how a single pathway is involved in the development of different tissues, but also its pleiotrophic role in tumorigenesis.

Methods

Mice. The experiments on mice were approved by the local animal experimental committee of the Leiden University and by the Commission Biotechnology in Animals of the Dutch Ministry of Agriculture (permission number VVA/BD 01.168).

Constructs. The gene-targeting Rosa26-β-geo construct used to tag wildtype ES cells by homologous recombination fused the ubiquitously expressed protein encoded by the endogenous Rosa26 locus with a hybrid β-galactosidase–neomycin-resistance protein (β-geo). The construct was a derivative of the gene trap construct previously employed[18] and was constructed and kindly provided by J.-H. Dannenberg and H. te Riele.

ES cell lines. We mated heterozygous $Apc^{+/1638N}$ and $Apc^{+/Min}$ mice on a mixed C57BL/6J × CD1 background and harvested blastocysts 3.5 d after fertilization. We plated the flushed pre-implantation blastocysts in 96-well dishes coated with mouse embryonic fibroblasts and cultured them to isolate undifferentiated ES-cell lines according to previously reported methods[20]. We obtained six independently isolated $Apc^{Min/Min}$,

four Apc$^{1638N/1638N}$, four littermate *Apc*$^{+/Min}$ and two wildtype *Apc*$^{+/+}$ ES-cell lines, which we used in the differentiation experiments. Only early passage (p4–p5) embryo-derived ES-cell lines were used. All remaining cell lines (*Apc*$^{1638N/1638N}$, *Apc*$^{1638N/1638T}$, *Apc*$^{1572T/1638N}$, *Apc*$^{1638T/1638T}$) were derived by gene targeting in the E14 ES-cell line (129/Ola), as previously described[9]. These cell lines were previously established and are therefore characterized by higher passage numbers (roughly p20). To exclude that the observed defects result from mutations acquired *in vitro*, at least two independently generated clones for each genotype were used in the teratoma assays.

We generated the *Catnb*$^{lox(ex3)}$ and *Catnb*^{ex3} ES-cell lines by *lox*P gene targeting and by Cre-mediated deletion of exon 3 as previously described[22].

Generation of teratomas. We prepared single-cell suspensions from semi-confluent undifferentiated ES-cell cultures grown on 9-cm culture dishes coated with mouse embryonic fibroblasts using 1× trypsin/EDTA (Life Technologies). We washed cells three times with a large volume of phosphate-buffered saline (PBS) and then injected subcutaneously a total of 4×10^6 cells in 200 µl PBS into the flank of a syngenic mouse. C57BL/6J × CD1 recipient mice were used for the blastocyst-derived ES-cell lines (*Apc*^{1638N} and *Apc*^{Min}). We injected ES cells with mutations in *Apc* or *Catnb* derived by gene targeting in the E14 ES-cell line[9,22] into 129/Ola recipient mice. Chimeric teratomas were induced by mixing 2×10^6 cells of each cell line shortly before injection. After 3 wk, the mice were killed and teratomas were removed, washed with PBS, fixed overnight in 4% paraformaldehyde and processed for paraffin-based histology using standard techniques.

Western-blot and immunoprecipitation analyses. To detect the various mutant Apc proteins by western-blot analysis, we derived total protein lysates and immunoprecipitates from freshly cultured ES-cell lines and resolved them on agarose gels as described previously[9]. We quantified residual amounts of the Apc1638 protein by mixing homozygous Apc^{1638N} ES cells with given percentages of wildtype ES cells before immunoprecipitation with the polyclonal antibody to N-terminal Apc (AFPN; ref. 9), immunoblotting and detecting product with a monoclonal antibody against Apc (Ab-1, Oncogene Research Products) recognizing amino acids 1–29 of Apc.

***In vitro* differentiation of ES cells.** We plated 10^4 ES cells per well on 12-well tissue culture plates and cultured them in ES culture medium containing LIF (Life Technologies) for 2 d. Spontaneous differentiation was allowed by keeping the ES clones in culture for 2 d in the presence and for 6 d in the absence of LIF without passaging. We induced differentiation by plating 2-d-old embryoid bodies on gelatin-coated 12-well culture plates and withdrawing LIF. We achieved differentiation to mesodermal, neuroectodermal and trophectodermal lineages by adding dimethyl sulfoxide (0.05%, 0.1%, 0.5%, 1% or 2%), retinoic acid (0.1 and 0.5 µM, Sigma) and fibroblast growth factor 4 (25 ng ml^{-1}), respectively, as previously described[19,20].

Immunohistochemical analysis of ES-cell colonies differentiated *in vitro*. Differentiated embryoid bodies attached to 12-well dishes were fixed with 1% paraformaldehyde for 10 min, washed for 5 min in PBS, dehydrated in methanol and stored at –20 °C until use. For immunohistochemistry, plates were re-hydrated in PBS and blocked in 5% non-fat dried milk (NFDM) in PBS for 2 h at room temperature. The primary antibody was diluted in 5% NFDM 2 h before use. We incubated samples with the primary antibody at 4 °C overnight under gentle shaking. The next day, we washed the plates five times for 30 min at room temperature with PBS containing 0.1% Tween-20 (PBT), after which the plates were incubated overnight with the secondary antibody diluted in PBS containing 5% NFDM. The following day we washed the plates thoroughly with PBT, equilibrated them in alkaline phosphatase buffer for 15 min and stained them with 5-bromo-4-chloro-3-indolyl phosphate and nitro blue tetrazolium according to the manufacturer's recommendations (Roche).

Antibodies. The primary antibodies used for immunohistochemistry were: mouse antibody against β-catenin (Transduction Laboratories), antibody against AFP (Novocastra), antibody against NCAM (5B8, from Developmental Studies Hybrydoma Bank (DSHB)), antibody against neurofilament (2H3, DSHB), antibody against synaptic vesicles (SV-2, DSHB), antibody against GFAP (DAKO), antibody against smooth muscle actin (clone 1A4, Neomarkers Ab-1), antibody against striated muscle (A4.1025, DSHB), antibody against vimentin (NCL-VIM, Novocastra) and antibody against α-fetoprotein (AFP 08-0055, Zymed Labs). The polyclonal antibody against AFPN was previously described[9].

For conventional immunohistochemistry and western-blot analysis, we used a goat antibody against mouse IgG/IgM conjugated with peroxidase. We used a goat antibody against mouse IgG/IgM conjugated with alkaline phosphatase as the secondary antibody for the immunohistochemical analysis of ES cells differentiated *in vitro*. All secondary antibodies were purchased from Jackson ImmunoResearch Laboratories.

TOPFLASH and FOPFLASH reporter assays. Twenty hours before transfection, we plated 10^5 cells per well on 12-well tissue culture plates coated by a feeder cell layer. We transfected cells in each well with 500 ng pTOPFLASH or pFOPFLASH vector (kindly provided by H. Clevers) and 500 ng *lacZ* vector (or 25 ng luciferase from *Renilla reniformis*) using Lipofectamine 2000 (Life Technologies) as recommended by the manufacturer. After 24 h, we measured luciferase activities in a luminometer (Lumat LB 9507) and normalized the data for the transfection efficiency by either measuring the β-galactosidase activity as described previously[9] or using the Dual Luciferase Reporter Assay system (Promega) according to the manufacturer's instruction.

Expression profiling by oligonucleotide microarray and data analysis. We extracted total RNA (200 µg) from snap-frozen teratomas by standard procedures. We isolated the poly(A)$^+$ fraction (roughly 2 µg) by Dynabeads biomagnetic separation (Dynal Biotech) and used them to directly probe the GeneChip Murine Genome U74A Set microarray (Affymetrix) according to the manufacturer's protocol.

We analyzed the microarray data using the Rosetta Resolver v3.0 Gene Expression Data Analysis System. The input data for the system were the CEL files generated by Affymetrix GeneChip. The CEL files contained the 75th percentile pixel intensity of a given feature as well as the standard deviation (s.d.) of the pixels and the number of pixels of a given feature. The Affymetrix array contained perfect match (PM) and corresponding mismatch probes (MM), which were used to control for background and non-specific hybridization. The arrays generally contained 16 probe pairs per probe set.

We processed the data by an error model in Rosetta Resolver v3.0 Gene Expression Data Analysis System. The error-weighted PM/MM differences were considered outliers and not used for computation if they were more than 3 s.d. from the mean of the PM/MM intensity difference for a given probe set.

If a probe pair was excluded on one array, then it was also excluded from the differential calculation between two arrays. We determined differential expression by correcting for intra-array gain adjustment, normalizing between arrays and correcting for non-linearity. The intra-array gain adjustment was calculated by dividing the array into 64 sectors and providing gain adjustments for each sector. For differential expression between two arrays, the sectors of the two arrays were normalized sector-by-sector. Then we detected a set of invariant probe sets by calculating the error-weighted log ratio between the two arrays. We used these probe sets, whose probe pairs exhibited a $\log_{10}$ ratio closest to zero, for the non-linearity adjustment. We calculated a *P* value for each probe set using the error-normalized differential expression between arrays. The error model assumed that the log ratio statistic followed a normal distribution. We used a probability density function of the error-normalized differential with the null hypothesis that the sequence was not differentially expressed.

We used the agglomerative clustering algorithm for clustering genes and arrays into a hierarchical structure. The error-weighted correlation without mean subtraction, based on log ratio, was used as the similarity measure. When merging the two closest objects, we used a heuristic criterion of average linkage to redefine the between-cluster similarity measure. Only sequences that had a factor of change = 2 and $P < 0.01$ were used for clustering. The color displays in Fig. 6*a* represent the $\log_{10}$ ratio between the two arrays, red when the sequence was upregulated relative to the control, green when downregulated and black when the expression was close to zero.

Acknowledgments

We thank J. Boer and collaborators from the Leiden Genome Technology Center for their assistance with the Affymetrix equipment and G.J.B. van Ommen for his continued support. This study was made possible by a grant to R.F. from the Dutch Research Council. M.R. was supported by grants from the Academy of Finland and the Finnish Cultural Foundation.

Competing interests statement

The authors declare that they have no competing financial interests.

Received 9 July; accepted 19 September 2002.

1. Cadigan, K.M. & Nusse, R. Wnt signaling: a common theme in animal development. *Genes Dev.* **11**, 3286–3305 (1997).
2. Seidensticker, M.J. & Behrens, J. Biochemical interactions in the wnt pathway. *Biochim. Biophys. Acta* **1495**, 168–182 (2000).
3. Polakis, P. Wnt signaling and cancer. *Genes Dev.* **14**, 1837–1851 (2000).
4. Kinzler, K.W. & Vogelstein, B. Lessons from hereditary colorectal cancer. *Cell* **87**, 159–170 (1996).
5. Fodde, R., Smits, R. & Clevers, H. *APC*, signal transduction and genetic instability in colorectal cancer. *Nature Rev. Cancer* **1**, 55–67 (2001).
6. Fodde, R. & Smits, R. Disease model: familial adenomatous polyposis. *Trends Mol. Med.* **7**, 369–373 (2001).
7. Su, L.K. *et al*. Multiple intestinal neoplasia caused by a mutation in the murine homolog of the *APC* gene. *Science* **256**, 668–670 (1992).
8. Moser, A.R. *et al*. Homozygosity for the Min allele of *Apc* results in disruption of mouse development prior to gastrulation. *Dev. Dyn.* **203**, 422–433 (1995).
9. Smits, R. *et al*. Apc1638T: a mouse model delineating critical domains of the adenomatous polyposis coli protein involved in tumorigenesis and development. *Genes Dev.* **13**, 1309–1321 (1999).
10. Fodde, R. *et al*. A targeted chain-termination mutation in the mouse *Apc* gene results in multiple intestinal tumors. *Proc. Natl Acad. Sci. USA* **91**, 8969–8973 (1994).
11. Smits, R. *et al*. Apc1638N: a mouse model for familial adenomatous polyposis-associated desmoid tumors and cutaneous cysts. *Gastroenterology* **114**, 275–283 (1998).
12. Fodde, R. & Khan, P.M. Genotype–phenotype correlations at the adenomatous polyposis coli (*APC*) gene. *Crit. Rev. Oncog.* **6**, 291–303 (1995).
13. Korinek, V. *et al*. Depletion of epithelial stem-cell compartments in the small intestine of mice lacking Tcf-4. *Nature Genet.* **19**, 379–383 (1998).
14. Boman, B.M., Fields, J.Z., Bonham-Carter, O. & Runquist, O.A. Computer modeling implicates stem cell overproduction in colon cancer initiation. *Cancer Res.* **61**, 8408–8411 (2001).
15. Korinek, V. *et al*. Constitutive transcriptional activation by a β-catenin–Tcf complex in $APC^{-/-}$ colon carcinoma. *Science* **275**, 1784–1787 (1997).
16. Stevens, L.C. The biology of teratomas. *Adv. Morphog.* **6**, 1–31 (1967).
17. Hay, E.D. & Zuk, A. Transformations between epithelium and mesenchyme: normal, pathological, and experimentally induced. *Am. J. Kidney Dis.* **26**, 678–690 (1995).
18. Friedrich, G. & Soriano, P. Promoter traps in embryonic stem cells: a genetic screen to identify and mutate developmental genes in mice. *Genes Dev.* **5**, 1513–1523 (1991).
19. Tanaka, S., Kunath, T., Hadjantonakis, A.K., Nagy, A. & Rossant, J. Promotion of trophoblast stem cell proliferation by FGF4. *Science* **282**, 2072–2075 (1998).
20. Rudnicki, M.A. & McBurney, M.W. Cell culture methods and induction of differentiation of embryonal carcinoma cell lines. in *Teratocarcinomas and Embryonic Stem Cells: A Practical Approach* (ed. Robertson, E.) 19–50 (IRL, Oxford, UK, 1987).
21. Kim, K., Pang, K.M., Evans, M. & Hay, E.D. Overexpression of β-catenin induces apoptosis independent of its transactivation function with LEF-1 or the involvement of major G1 cell cycle regulators. *Mol. Biol. Cell* **11**, 3509–3523 (2000).
22. Harada, N. *et al*. Intestinal polyposis in mice with a dominant stable mutation of the β-catenin gene. *EMBO J.* **18**, 5931–5942 (1999).
23. Urist, M.R. Bone: formation by autoinduction. *Science* **150**, 893–899 (1965).
24. Wozney, J.M. *et al*. Novel regulators of bone formation: molecular clones and activities. *Science* **242**, 1528–1534 (1988).
25. Hollnagel, A., Oehlmann, V., Heymer, J., Ruther, U. & Nordheim, A. Id genes are direct targets of bone morphogenetic protein induction in embryonic stem cells. *J. Biol. Chem.* **274**, 19838–19845 (1999).
26. Hu, G., Lee, H., Price, S.M., Shen, M.M. & Abate-Shen, C. *Msx* homeobox genes inhibit differentiation through upregulation of cyclin D1. *Development* **128**, 2373–2384 (2001).
27. Chen, J. *et al*. Microarray analysis of Tbx2-directed gene expression: a possible role in osteogenesis. *Mol. Cell. Endocrinol.* **177**, 43–54 (2001).
28. Yamada, M., Revelli, J.P., Eichele, G., Barron, M. & Schwartz, R.J. Expression of chick *Tbx-2*, *Tbx-3*, and *Tbx-5* genes during early heart development: evidence for BMP2 induction of Tbx2. *Dev. Biol.* **228**, 95–105 (2000).
29. Monaghan, A.P. *et al*. Dickkopf genes are co-ordinately expressed in mesodermal lineages. *Mech. Dev.* **87**, 45–56 (1999).
30. Fodde, R. *et al*. Mutations in the *APC* tumour suppressor gene cause chromosomal instability. *Nature Cell Biol.* **3**, 433–438 (2001).
31. Morin, P.J. *et al*. Activation of β-catenin–Tcf signaling in colon cancer by mutations in β-catenin or APC. *Science* **275**, 1787–1790 (1997).
32. Lamlum, H. *et al*. The type of somatic mutation at *APC* in familial adenomatous polyposis is determined by the site of the germline mutation: a new facet to Knudson's 'two-hit' hypothesis. *Nature Med.* **5**, 1071–1075 (1999).
33. Smits, R. *et al*. Somatic *Apc* mutations are selected upon their capacity to inactivate the β-catenin downregulating activity. *Genes Chromosomes Cancer* **29**, 229–239 (2000).
34. Shih, I.M. *et al*. Top-down morphogenesis of colorectal tumors. *Proc. Natl Acad. Sci. USA* **98**, 2640–2645 (2001).
35. Moser, A.R., Dove, W.F., Roth, K.A. & Gordon, J.I. The Min (multiple intestinal neoplasia) mutation: its effect on gut epithelial cell differentiation and interaction with a modifier system. *J. Cell Biol.* **116**, 1517–1526 (1992).
36. Ryo, A., Nakamura, M., Wulf, G., Liou, Y.C. & Lu, K.P. Pin1 regulates turnover and subcellular localization of β-catenin by inhibiting its interaction with APC. *Nature Cell Biol.* **3**, 793–801 (2001).

erratum

Functional SNPs in the lymphotoxin-α gene that are associated with susceptibility to myocardial infarction

K Ozaki, Y Ohnishi, A Iida, A Sekine, R Yamada, T Tsunoda, H Sato, H Sato, M Hori, Y Nakamura & T Tanaka

Nat. Genet. **32**, 650–654 (2002).

Published online 11 November 2002; doi:10.1038/ng1047

A typographical error in the third sentence of the abstract resulted in the *P* value for the association being incorrectly reported as $P = 0.00000033$. The correct value is, in fact, $P = 0.0000033$.

corrigendum

Apc modulates embryonic stem-cell differentiation by controlling the dosage of β-catenin signaling

M F Kielman, M Rindapää, C Gaspar, N van Poppel, C Breukel, S van Leeuwen, M M Taketo, S Roberts, R Smits & R Fodde

Nat. Genet. **32**, 594–605 (2002).

Published online 11 November 2002; doi:10.1038/ng1045

The name of the second author was misspelled. The correct spelling is Maaret Ridanpää.